NANOSYSTEMS: PHYSICS, CHEMISTRY, MATHEMATICS, 2015, 6 (3), P. 320–331

Storage and separation of CO_2 and CH_4 in boron imidazolate frameworks: a theoretical study from Monte Carlo simulation

B. Assfour*[1,2], S. Leoni[1]

[1]Institut für Physikalische Chemie, Technische Universität Dresden, 01062 Dresden, Germany

[2]Department of Chemistry, Atomic Energy Commission, P.O. Box 6091, Damascus, Syria

cscientific@aec.org.sy

PACS 87.15.ag **DOI 10.17586/2220-8054-2015-6-3-320-331**

In this work, the storage of pure CO_2 and CH_4 gases and separation of their binary mixture in new type of nanostructured materials called boron imidazolate frameworks (BIFs) have been investigated using atomistic simulation to provide information for material selection in adsorbent designs. Adsorption isotherms and adsorption selectivities were computed using grand canonical Monte Carlo (GCMC). Our results showed that BIFs exhibit significantly higher selectivities for separation of CO_2 from CH_4 compared to other widely studied metal organic framework (MOF) materials.

Keywords: Adsorption, MOFs, BIFs, Gas Separation and Selectivity.

Received: 3 March 2015

Revised: 30 March 2015

1. Introduction

The continued combustion of fossil fuel causes a rapid increase in the concentration of carbon dioxide (CO_2) in earth's atmosphere, which is believed to be responsible for global warming and climate change [1]. In order to avoid CO_2 from reaching the atmosphere, the capture of CO_2 and the utilization of a clean energy source are prominent. Methane, the primary component of natural gas, is an appealing energy source. Compared to gasoline, methane provides much more energy because of its higher hydrogen-to-carbon ratio, and has much lower CO_2 emissions [2]. However, the practical storage of methane in automobiles is still a prime challenge. According to U.S. Department of Energy (DOE) requirements, the storage capacity of material-based adsorbed methane should exceed 180 cm^3 (STP). cm^{-3} at 298 K and 35 bar for practical on-board methane storage, where cm^3 (STP).cm^{-3} means standard temperature and pressure equivalent volume of methane per volume of the adsorbent material. In term of energy density, this is equivalent to methane compressed at 250 bar and room temperature [3].

In parallel to the environmentally friendly fuel research, a large amount of work has been focused on the development of novel techniques for the separation, capture, and storage of CO_2. The former is a key step in carbon sequestration for the prevention of global warming. Furthermore, CO_2 is an impurity in natural gas, biogas and syngas [4]. Its presence will reduce the overall energy content of gas streams. Therefore, beside the storage of pure CO_2 and CH_4 components, it is of large importance to separate their mixtures. One promising method for separation of CO_2 from its mixtures is adsorption separation by nanoporous materials. Among the potential adsorbent candidates (i.e. zeolites, activated carbon and

so on) [5,6], metal organic frameworks (MOFs) have emerged as a front-runner. MOFs are ultra-porous crystalline materials that are able to trap and store voluminous amounts of gas molecules (i.e. CH_4, H_2, N_2 and CO_2) [7]. The fact that the structure of MOFs can be tailored and chemically functionalized to selectively adsorb specific gas in a mixture gives them an enormous advantage over other nanoporous materials. Furthermore, MOFs have a versatile ability to store and release gases with fast kinetics and high reversibility over multiple cycles.

Boron imidazolate frameworks (BIFs) [8], a novel subclass of MOFs, are considered as promising materials for hydrogen storage applications [9]. Unlike the zinc imidazolate system (ZIFs), BIFs contain light chemical elements (i.e. Li and B) as framework vertices linked by different imidazolate ligands (im). The coordinatively unsaturated centers presented in BIFs have been shown to be favorable for enhancing gas uptake capacity [10]. Recently, Yang *et al.* have prepared novel neutral boron–imidazolate-framework (BIF-35) based on the assembly of tetradentate $B(im)_4$ ligands and (CdBr) units, illustrating the ability to include a much wider variety of metal ions than traditional tetrahedral metal centers in order to produce new BIFs [11].

In contrast to the extensive studies on other MOFs, investigations of BIFs are rather limited. Zheng and co-workers integrated metal carboxylates and boron imidazolates to prepare a novel family of BIFs called MC-BIFs [12]. Amongst these materials, MC-BIF-2H exhibits extraordinary volumetric capacity for storing CO_2 (81 L/L at 273 K and ambient pressure), comparable to that previously reported for a highly porous ZIF-69 (83 L/L) [13]. Zhang *et al.* developed a new strategy for the design of zeolite-type MOFs. They successfully synthesized the first interrupted zeolite A (4-connected tetrahedral framework) with a 3-connected network denoted as BIF-20. The initial H_2 uptake of BIF-20 is remarkably high. However, The CO_2 uptake capacity (34.8 cm^3/g under ambient condition) is comparable to that reported for other ZIFs [14]. Wang *et al.* synthesized new set of BIFs with ACO and ABW topologies. The ACO-type material shows interesting gas selectivity of CO_2 over N_2 and CH_4 [15]. Recently, Zang and co-workers [16] reported highly porous *ctn*-type BIF material with high CO_2 storage capacity (104.3 cm^3/g at 273 K). Moreover, this material presents high selectivity for the adsorption of CO_2 over CH_4 at ambient conditions. Jayaramulu *et al.* have synthesized a new three-dimensional boron based MOF, and made use of it as a precursor to produce a borocarbonitride (BC_4N). Besides having an unusual coral-like morphology, BC_4N has a high BET surface area (988 m^2/g) and exhibits significant CO_2 and H_2 uptake [17].

Complementary to experimental studies, a number of computational investigations of gas adsorption in various types of nanoporous compounds have been reported. Most of these studies investigated the chemical structure, network topology, and porosity effects on the adsorption properties of the materials [18-20].

In this paper, we extend our previous work on BIFs by using molecular modeling to examine CO_2 storage and separation (relative to CH_4) in series of BIFs with different topologies. The results of this work may provide useful information for unlocking the potential of these materials in storage and separation applications and help the design of new adsorbents with improved properties by studying the effect of topology on CO_2 adsorption. The crystal structures of these materials are shown in Fig 1. For a description of topology symbols, see the Database of Zeolite Structures, http://www.iza-structure.org/databases/.

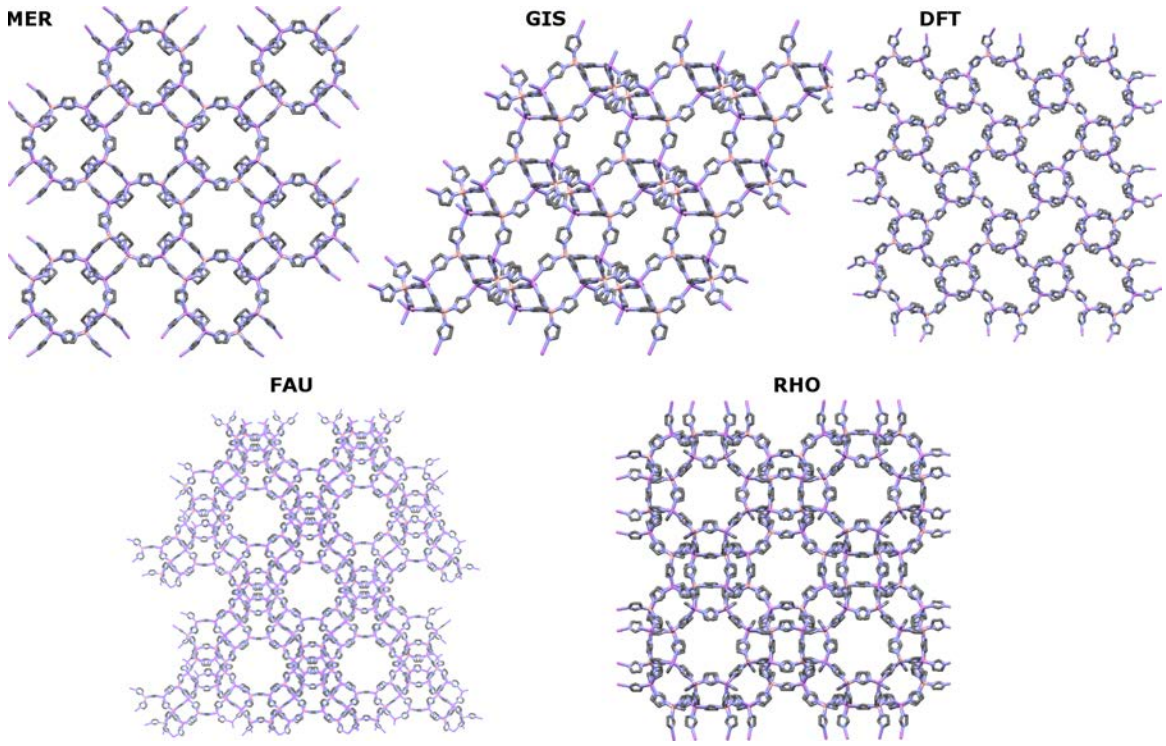

FIG. 1. Crystal structures of the MOFs studied in this work. The structures are not drawn to scale. B:pink, C: grey, N:blue, Li: cyan. Hydrogen atoms are omitted for clarity

2. Model

The methane and carbon dioxide adsorption and separation in BIF structures were simulated with the grand canonical Monte-Carlo (GCMC) method using the multipurpose simulation code MUSIC [21]. The code MUSIC was successfully used to simulate the adsorption of different gases, such as CH_4, CO_2 and H_2, on a variety of nanoporous materials [22-26]. In the grand canonical ensemble, the chemical potential, temperature and volume are constant. The chemical potential was converted to fugacity using Peng–Robinson equation of state [27]. The intermolecular interactions were modeled by the Lennard-Jones pair potential between all sites to represent van der Waals interactions. A methane molecule is modeled as united atom, where potential parameters are taken from Goodbody *et al.* [28]. The carbon dioxide molecule is modeled using TraPPe force field [29]. In this model, the CO_2 is treated as three-site liner molecule, where the C-O bond measures 1.16 Å. This model can reproduce the experimental gas-phase quadrupole moment of carbon dioxide by placing partial charges on C ($+0.70$ e) and O (-0.35 e) atoms. The potential parameters of BIF atoms were taken from the universal force field (UFF) of Rappe *et al.* [30], which has been widely used to study the adsorption of different gases on nanoporous materials [23, 31-33]. Lorentz-Berthelot mixing rules were used to calculate mixed Lennard-Jones parameters. The electrostatic interactions between CO_2 molecules and the BIF structure were accounted for by placing point charges on each atom. The Bader partitioning scheme was performed on electronic density with the program Dgrid [34] to calculate the charge on individual atoms. The electronic density was calculated with the all-electron, full-potential local orbital (FPLO) minimal basis method [35]. The FPLO method does not have any atomic (or muffin–tin) spheres so that the whole space is treated in a uniform manner. The atomic

charges were calculated for zni topology, and kept permanent from structure to structure. The Ewald summation technique is used to calculate the electrostatic interactions.

The simulation box, representing each BIF structure, contains 8 (2×2×2) unit cells. Adsorbents were treated as rigid with atom positions taken from Ref [36]. The periodic boundary conditions were employed in all dimensions to mimic the crystalline periodicity. Interactions beyond 13 $\AA$ were neglected. Each simulation point consisted of 5×10^6 Monte-Carlo steps to reach equilibrium followed by an extra 5×10^6 steps to take the statistical average.

GCMC simulation delivers the absolute amount adsorbed (N_{abs}), whereas experiments give the excess amount of adsorption (N_{ex}). In order to make the comparison, the excess amount should be converted into absolute as:

$$N_{\mathrm{ex}} = N_{\mathrm{abs}} - \rho_{\mathrm{p}} V_{\mathrm{free}} \tag{1}$$

where $\rho_p$is the density of the bulk phase [37], and V_{free} is the is the available pore volume per unit cell of the sorbent estimated using a non-adsorbing species (helium) as a probe [23, 25, 26].

The accessible surface area was calculated by "rolling" a probe molecule with a diameter equal to the Lennard–Jones parameter for N_2 (3.681 $\AA$) over the framework's surface as described in Ref [38]. Calculation of the isosteric heat of adsorption (Q_{st}) at zero coverage was performed through the fluctuations over the internal energy and from fluctuations of number of particles in the system by considering a very low pressure. These calculations are reported in more detail elsewhere [39].

In adsorption-based separation process, a good indication of the ability for separation is the adsorption selectivity for different components in gas mixture. The adsorption selectivity of component i relative to component j is defined by:

$$S = \frac{x_i/x_j}{y_i/y_j} \tag{2}$$

where x_i and x_j are the molar fractions of component i and j in adsorbed phase and y_i and y_j are the molar fractions in the gas phase.

3. Results and discussion

3.1. Adsorption of pure components of CH_4 and CO_2

Table 1 gives the density, pore volume and accessible surface area for all five BIFs as well as the initial isosteric heats of adsorption for pure CO_2 and CH_4 in each material. All materials provide moderate surface area and low density, indicating that they may be promising candidates for gas storage applications [2]. The material with FAU topology has the lowest density (0.492 g/cm^3) as well as the highest surface area (2773 m^2/g), which is higher than that of zeolites, porous silica and lower than some MOFs [40] or COFs [25]. As is the case for most CH_4 sorbents, the Q_{st} is in the range of 12–18 kJ.mol^{-1} [41-46]. However, for MOFs exhibiting very high methane uptake, such as PCN-14 [47], the Q_{st} is much larger (15–30 kJ.mol^{-1}), which is known to be responsible for the exceptionally high methane uptake at low pressure.

In the given material, the Q_{st} of CO_2 is larger than that of CH_4, indicating that CO_2 is more strongly adsorbed. Consequently, BIFs show more affinity toward CO_2 at lower pressures. This is expected because the CO_2 molecule has a greater interaction with the adsorbent than CH_4 because it contains three interaction sites plus the role of electrostatic

TABLE 1. Summary of calculated properties of different BIFs

Material	density (g/cm^3)	pore volume (cm^3/g)	accessible surface area for N_2	Initial Q_{st} for CH_4 (kJ/mol)	Initial Q_{st} for CO_2 (kJ/mol)
RHO	0.566	1.11	2654	12.15	38.52
FAU	0.492	1.41	2773	14.61	36.55
DFT	0.730	0.74	1686	17.33	49.93
GIS	0.627	0.97	2625	13.11	36.11
MER	0.635	0.95	2613	12.57	37.72

interactions, which is expected to be enhanced compared to other MOFs due to the asymmetries in the metal sites. The Q_{st} is in the range of 36–50 kJ.mol^{-1} higher than those for other MOFs, i.e. UiO-68(Zr) (20 kJ.mol^{-1}) [48], MOF-5 (34 kJ.mol^{-1}) [49], CPO-27. (38–43 kJ mol^{-1}) [44]. For both CO_2 and CH_4, The Q_{st} is the largest in DFT. This is probably due to the lower porosity.

The predicted gravimetric methane uptakes in selected BIFs at 298 K are shown in Figure 2. As expected, all materials show type I for total and excess isotherms, with profiles that depend on the material. The material with DFT topology shows the highest excess uptake almost all over the pressure range. Its saturation uptake is calculated to be 248 cm^3/g at 40 bar, which is close to 252 cm^3/g (290 K, 35 bar) for PCN-14, which holds the current record for methane storage [47]. Although, recently Peng *et al.* [50] discovered that packed HKUST-1exhibits a room-temperature volumetric methane uptake that exceeds any value reported to date. The material with FAU topology shows a slightly higher saturation gravimetric uptake (254 cm^3/g) but at higher saturation pressure (70 bar). The total uptake that a material can store is more relevant to the practicability of using CH_4 as a fuel. In terms of total methane uptake, the best material at 100 bar is the one with FAU topology, with 405 cm^3/g followed by GIS and RHO (336 cm^3/g) and DFT (306 cm^3/g) respectively.

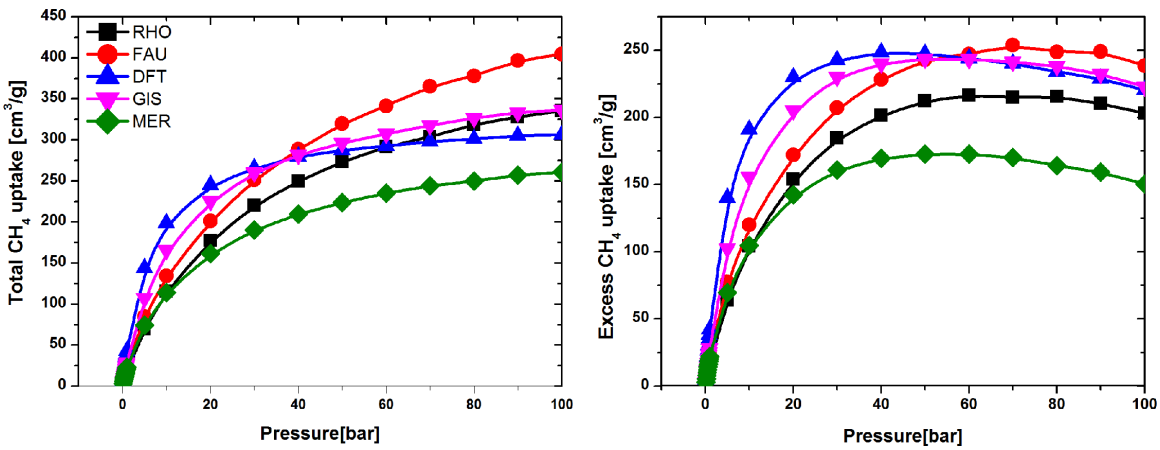

FIG. 2. Excess and total gravimetric CH_4 uptake in BIFs

Concerning the volumetric uptake (Figure 3), we see that all BIFs materials do not reach the DOE target in a total volumetric uptake basis at 35 bar. However, we predict that materials with FAU and RHO topologies perform nicely, having uptakes of 200 and

190 v(STP)/v at 100 bar, respectively, suggesting that they could be suitable for practical applications of methane storage.

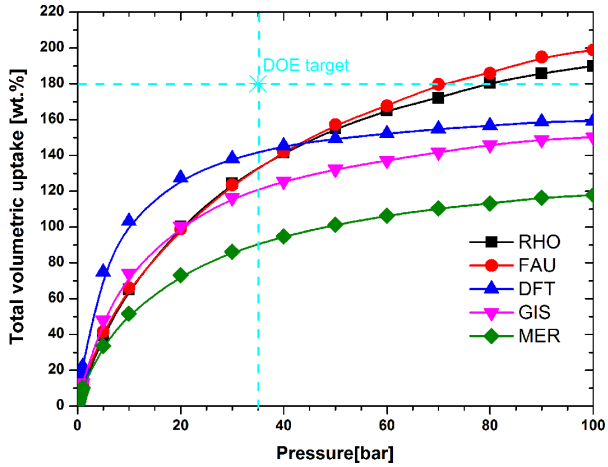

FIG. 3. Total volumetric CH_4 uptake in BIFs

High and low pressure CO_2 isotherms for all five BIFs were calculated and are presented in Figure 4. Unlike the CH_4 isotherm, CO_2 isotherms show dramatic steps, similar to those reported for CO_2 in other MOFs [32, 51-53] indicating a very high affinity for CO_2 gas. Compared with other porous materials [22, 54], BIFs reach their saturation uptakes at relatively low pressures (around 10 bar). The material with FAU topology shows the highest excess and total uptake (figure 4) almost over the entire pressure range. The total CO_2 storage capacity for FAU at 50 bar reaches the value of 450 mg.g^{-1}. Such value is significantly lower than those reported for other recently synthesized materials such as MOF-200 (2400 mg.g^{-1}) and NU-100 (2315 mg.g^{-1}). This is due to very large pore volumes provided by these materials, where the amounts of CO_2 uptake are directly related to the total pore volume [54]. However, BIFs present very high CO_2 capacities at low pressure range (left panel of figure 4). For instance the calculated excess capacity of FUA at 1 bar (298 mg.g^{-1}) is almost three times higher than that reported for NU-100 (110 mg.g^{-1}) under the same conditions [22] and more than 50% greater than that of ZIF-69 (130 mg.g^{-1}) at 273 K, which makes this type of materials very promising candidates for CO2 capture, especially at low pressures.

3.2. Adsorption of CO_2/CH_4 mixture

In this section, the CO_2 selectivity for CO_2/CH_4 mixtures with different pressures at room temperature is discussed. Figure 5 shows the adsorption isotherms for an equimolar mixture of CH_4/CO_2 in BIFs as a function of pressure. We find that in all BIFs, CO_2 is more readilly adsorbed than CH_4 at low pressures (below 10 bar). This is due to stronger interaction with structures as explained above. However, at high pressures, the number of CH_4 molecules adsorbed per unit cell increases exponentially and CH_4 become more favorably adsorbed.

Figure 5 (right bottom) illustrates the effect of pressure on the CO_2 selectivity at room temperature for five BIFs. It shows that selectivities for CO_2 are different between BIFs at low pressures with the order RHO > FAU > GIS > DFT > MER. It can be seen that selectivities decrease exponentially along with rising pressure and become close at pressures

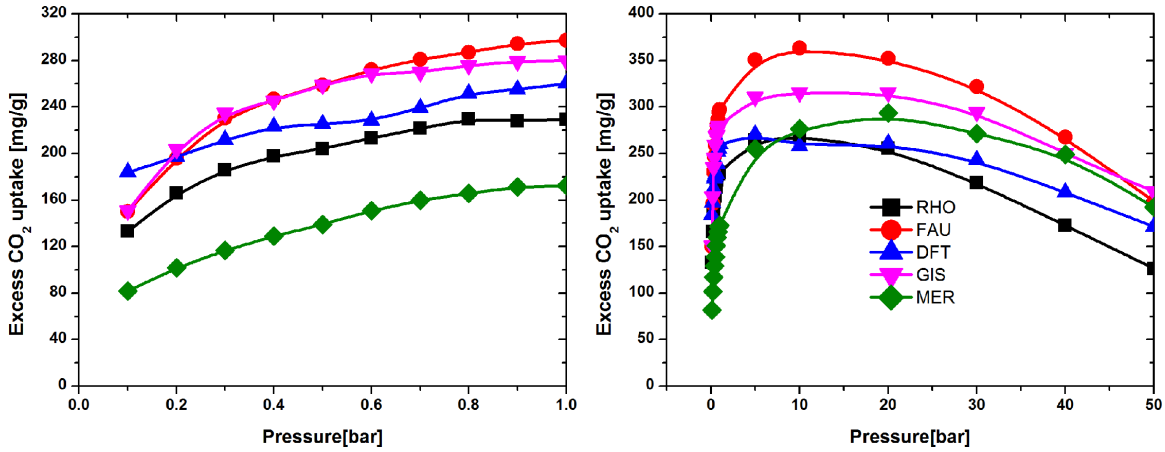

FIG. 4. Low (left) and high (right) excess gravimetric CO_2 uptake in BIFs

higher than 1.0 bar. Therefore, we conclude that the topology of BIFs plays the main role on the CO_2 selectivity rather than pressure.

Keskin studied the adsorption selectivities of ZIF type materials for equimolar CO_2/CH_4 mixture [55]. Results showed that adsorption selectivities of ZIFs are better than those of IRMOFs due to their smaller pore sizes and better confinement of CO_2 molecules. In contrast to BIFs, the selectivities for ZIFs increase with pressure. ZIF-3 (DFT topology) provides the best selectivity with 5 at 0.1 bar and up to 12 at 50 bar, whereas, for BIFs, RHO has the maximum selectivity with 50 at 0.1 bar down to almost 0 at 50 bar. Therefore, in sources such as flue gas, where the typical anticipated partial pressure of CO_2 is about 0.1 bar [56], BIFs outperform ZIFs and related MOFs because of their suitable pore sizes. However, at high pressures MOFs are better for CO_2 capture because of their larger pore sizes. This makes BIFs very promising candidates for CO_2 separation at low pressures.

4. Preferential adsorption sites

To understand the adsorption mechanism for CH_4 and CO_2 on BIFs, preferential adsorption sites were investigated. Since the picture of adsorption sites for all BIFs is similar, we choose DFT BIF as a representative. Figure 6 shows equilibrium snapshots of adsorbed CH_4/CO_2 mixture in the simulation unit cell at three different pressures, 0.1, 1.0, and 10 bar. It is clear that CO_2 molecules preferentially adsorb in the small pores formed by imidazole linkers (figure 7 (a)), while CH_4 molecules cannot enter the small pores because their sizes are smaller than the kinetic diameter of CH_4. Therefore CH_4 molecules are accommodated in the large pore. With increasing pressure, the CO_2 molecules also adsorb in large pores near to the polar centers in the framework because the electrostatic contribution of CO_2 is larger than that of CH_4 (figure 7 (b)). At higher pressures, the adsorption sites are saturated and the electrostatic interaction decreases to a negligible value. Therefore, CO_2 molecules are no longer favorable and together with CH_4 molecules, fill in the free space in the pores far from the charge centers. This behavior explains the large uptake of CO_2 at low pressure.

Generally, in separation processes, the differences in electronic properties and size of molecules are used. However, the relatively small difference in kinetic diameters between CO_2 (3.30 $\AA$) and CH_4 (3.76 $\AA$) makes separation based solely on molecule size a very difficult task. Therefore, many MOFs with unsaturated metal sites were synthesized to enhance adsorption of quadrupolar CO_2 over non-quadrupolar CH_4 and to make the separation beneficial. Bae *et al.* [57] found that incorporation of Li cations into MOFs, by either chemical reduction

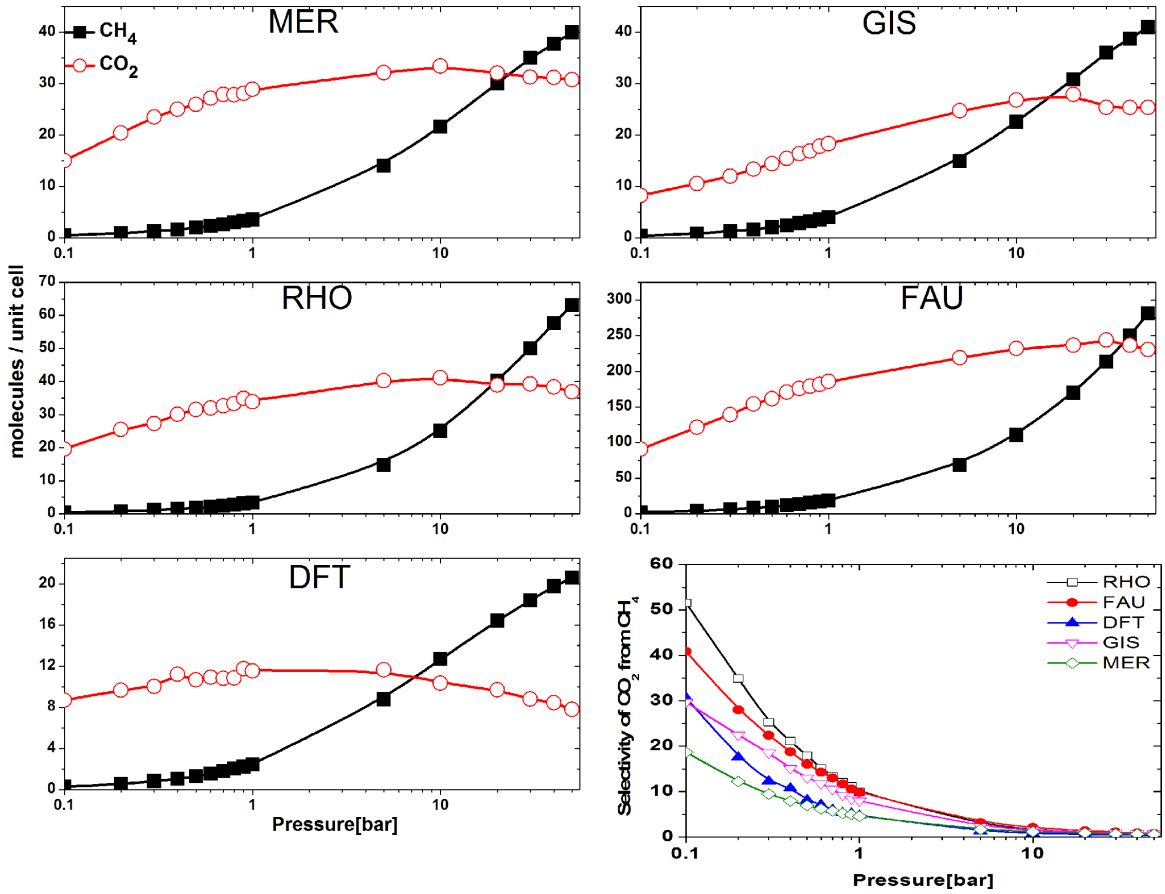

FIG. 5. Equimolar mixture adsorption isotherms of CH_4/CO_2in five BIFs. Adsorption selectivity of BIFs for CO_2/CH_4 mixture at room temperature (right bottom)

or cation exchange, significantly improved the CO_2/CH_4 selectivity. In case of BIFs both effects are presented, the unsaturated metal sites and optimal pore size. This may explain the large CO_2 uptake at low pressure relative to other MOFs.

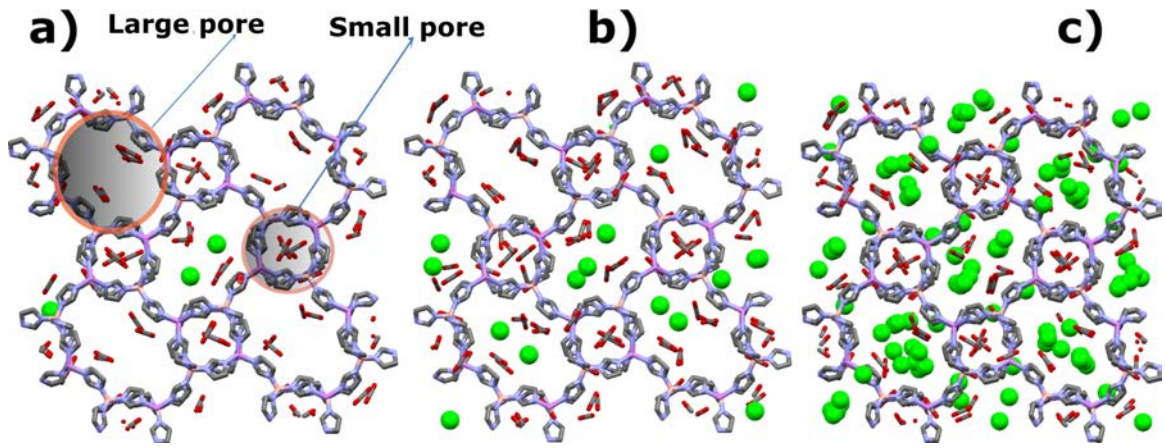

FIG. 6. Snapshots of mixture of CO_2 and CH_4 in DFT for low ((a) 0.1 bar), normal ((b) 1 bar), and intermediate ((c) 10 bar) loading. CH_4 molecules are represented in green

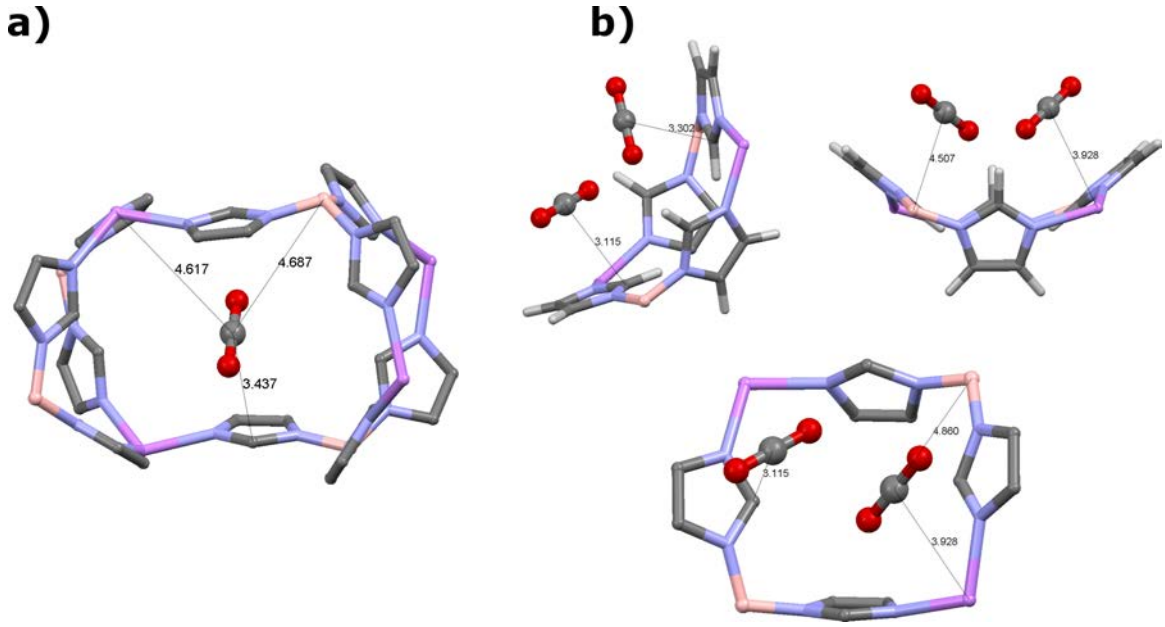

FIG. 7. CO_2 adsorption site in the small (a) and in the large cage (b). Distances are reported in angstroms

5. Conclusions

We have used computational modeling to study the storage and separation of CO_2 and CH_4 in a new class of porous materials known as BIFs. Our results show that BIFs could be suitable for practical applications of methane storage, particularly from a gravimetric point of view. We have also established that BIFs are highly selective for the absorption of CO_2 at low pressures as compared to other MOFs. Such high selectivities are believed to be the result of both appropriate pore sizes and unsaturated metal sites, which are known to significantly influence the CO_2 uptake capacity. The results of this work will provide guidelines for the optimum choice of BIF materials to be used in gas storage and separation applications.

Acknowledgments

The author is highly grateful to *Prof. Dr.* I.othman and Dr. Z.ajji for giving the opportunity and help performing this work.

References

[1] Haszeldine R.S. Carbon Capture and Storage. How Green Can Black Be? *Science*, 2009, **325**(5948), P. 1647-52.

[2] Duren T., Sarkisov L., Yaghi O.M., Snurr R.Q. Design of new materials for methane storage. *Langmuir*, 2004, **20**(7), P. 2683-9.

[3] Wegrzyn J., Gurevich M. *Appl Energy*, 1996, **55**, P. 71.

[4] Singh D., Croiset E., Douglas P.L., Douglas M.A. Techno-economic study of CO_2 capture from an existing coal-fired power plant: MEA scrubbing vs. O_2/CO_2 recycle combustion. *Energy Conversion and Management*, 2003, **44**(19), P. 3073-91.

[5] D'Alessandro D.M., Smit B., Long J.R. Carbon Dioxide Capture: Prospects for New Materials. *Angewandte Chemie International Edition*, 2010, **49**(35), P. 6058-82.

[6] Mulgundmath V.P., Tezel F.H., Saatcioglu T., Golden T.C. Adsorption and separation of CO_2/N_2 and CO_2/CH_4 by 13X zeolite. *The Canadian Journal of Chemical Engineering*, 2012, **90**(3), P. 730-8.

[7] Furukawa H., Cordova K.E., O'Keeffe M., Yaghi O.M. The Chemistry and Applications of Metal-Organic Frameworks. *Science*, 2013, **341**(6149).

[8] Zhang H., Wu T., Zhou C., Chen S.M., Feng P.Y., Bu X.H.. Zeolitic Boron Imidazolate Frameworks. *Angewandte Chemie-International Edition*, 2009, **48**(14), P. 2542-5.

[9] Baburin I.A., Assfour B., Seifert G., Leoni S. Polymorphs of lithium-boron imidazolates: energy landscape and hydrogen storage properties. *Dalton Transactions*, 2011, **40**(15), P. 3796-8.

[10] Horike S., Shimomura S., Kitagawa S. Soft porous crystals. *Nature Chem.*, 2009, **1**, P. 695-704.

[11] Yang E., Wang L., Zhang J. A luminescent neutral cadmium(ii)-boron(iii)-imidazolate framework with sql net. *CrystEngComm.*, 2014, **16**(14), P. 2889-91.

[12] Zheng S., Wu T., Zhang J., Chow M., Nieto R.A., Feng P., et al. Porous Metal Carboxylate Boron Imidazolate Frameworks. *Angewandte Chemie International Edition*, 2010, **49**(31), P. 5362-6.

[13] Banerjee R., Phan A., Wang B., Knobler C., Furukawa H., O'Keeffe M., et al. High-throughput synthesis of zeolitic imidazolate frameworks and application to CO_2 capture. *Science*, 2008, **319**(5865), P. 939-43.

[14] Zhang H.-X., Wang F., Yang H., Tan Y.-X., Zhang J., Bu X. Interrupted Zeolite LTA and ATN-Type Boron Imidazolate Frameworks. *Journal of the American Chemical Society*, 2011, **133**(31), P. 11884-7.

[15] Wang F., Shu Y.-B., Bu X., Zhang J. Zeolitic Boron Imidazolate Frameworks with 4-Connected Octahedral Metal Centers. *Chemistry – A European Journal*, 2012, **18**(38), P. 11876-9.

[16] Zhang H.-X., Fu H.-R., Li H.-Y., Zhang J., Bu X. Porous ctn-Type Boron Imidazolate Framework for Gas Storage and Separation. *Chemistry – A European Journal*, 2013, **19**(35), P. 11527-30.

[17] Jayaramulu K., Kumar N., Hazra A., Maji T.K., Rao C.N.R. A Nanoporous Borocarbonitride (BC_4N) with Novel Properties Derived from a Boron-Imidazolate-Based Metal–Organic Framework. *Chemistry – A European Journal*, 2013, **19**(22), P. 6966-70.

[18] Fischer M., Bell R.G. Interaction of hydrogen and carbon dioxide with sod-type zeolitic imidazolate frameworks: A periodic DFT-D study. *Cryst. Eng. Comm.*, 2014, **16**(10), P. 1934-49.

[19] Mellot-Draznieks C, Kerkeni B. Exploring the interplay between ligand and topology in zeolitic imidazolate frameworks with computational chemistry. *Molecular Simulation*, 2013, **40**(1-3), P. 25-32.

[20] Galvelis R., Slater B., Cheetham A.K., Mellot-Draznieks C. Comparison of the relative stability of zinc and lithium-boron zeolitic imidazolate frameworks. *Cryst. Eng. Comm.*, 2012, **14**(2), P. 374-8.

[21] Gupta A., Chempath S., Sanborn M.J., Clark L.A., Snurr R.Q. Object-oriented programming paradigms for molecular modeling. *Mol Simul.*, 2003, 29(1), P. 29-46.

[22] Farha O.K., Özgür Yazaydın A., Eryazici I., Malliakas C.D., Hauser B.G., Kanatzidis M.G., et al. De novo synthesis of a metal–organic framework material featuring ultrahigh surface area and gas storage capacities. *Nat Chem.*, 2010, **2**(11), P. 944-8.

[23] Assfour B., Seifert G. Hydrogen storage in 1D nanotube-like channels metal-organic frameworks: Effects of free volume and heat of adsorption on hydrogen uptake. *International Journal of Hydrogen Energy*, 2009, **34**(19), P. 8135-43.

[24] Bae Y.-S., Snurr R.Q. Optimal isosteric heat of adsorption for hydrogen storage and delivery using metal-organic frameworks. *Microporous and Mesoporous Materials*, 2010, **132**(1-2), P. 300-3.

[25] Assfour B., Seifert G. Adsorption of hydrogen in covalent organic frameworks: Comparison of simulations and experiments. *Microporous and Mesoporous Materials*, 2010, **133**(1-3), P. 59-65.

[26] Assfour B., Leoni S., Yurchenko S., Seifert G. Hydrogen storage in zeolite imidazolate frameworks. A multiscale theoretical investigation. *International Journal of Hydrogen Energy*, 2011, **36**(10), P. 6005-13.

[27] Peng D.-Y., Robinson D.B. A New Two-Constant Equation of State. *Industrial & Engineering Chemistry Fundamentals*, 1976, **15**(1), P. 59-64.

[28] Goodbody S.J., Watanabe K., MacGowan D., Walton J.P.R.B., Quirke N. Molecular simulation of methane and butane in silicalite. *Journal of the Chemical Society, Faraday Transactions*, 1991, **87**(13), P. 1951-8.

[29] Potoff J.J., Siepmann J.I. Vapor–liquid equilibria of mixtures containing alkanes, carbon dioxide, and nitrogen. *AIChE Journal*, 2001, **47**(7), P. 1676-82.

[30] Casewit C.J., Colwell K.S., Rappe A.K. Application of a universal force field to organic molecules. *Journal of the American Chemical Society*, 1992, **114**(25), P. 10035-46.

[31] Keskin S., Sholl D.S. Assessment of a Metal-Organic Framework Membrane for Gas Separations Using Atomically Detailed Calculations: CO_2, CH_4, N-2, H-2 Mixtures in MOF-5. *Industrial & Engineering Chemistry Research*, 2009, **48**(2), P. 914-22.

[32] Liu D.H., Zheng C.C., Yang Q.Y., Zhong C.L. Understanding the Adsorption and Diffusion of Carbon Dioxide in Zeolitic Imidazolate Frameworks: A Molecular Simulation Study. *Journal of Physical Chemistry C*, 2009, **113**(12), P. 5004-9.

[33] Morris W., He N., Ray K.G., Klonowski P., Furukawa H., Daniels I.N., et al. A Combined Experimental-Computational Study on the Effect of Topology on Carbon Dioxide Adsorption in Zeolitic Imidazolate Frameworks. *The Journal of Physical Chemistry C*, 2012, **116**(45), P. 24084-90.

[34] Kohout M. DGrid. 4.5 ed. Radebeul 2009.

[35] Koepernik K., Eschrig H. Full-potential nonorthogonal local-orbital minimum-basis band-structure scheme. *Physical Review B*, 1999, **59**(3), P. 1743-57.

[36] Baburin I.A., Assfour B., Seifert G., Leoni S. Polymorphs of lithium-boron imidazolates: energy landscape and hydrogen storage properties. *Dalton Transactions*, 2011.

[37] Webbook N.C. Available from: http://webbook.nist.gov/chemistry/fluid/.

[38] Düren T., Millange F., Ferey G., Walton K.S., Snurr R.Q. Calculating geometric surface areas as a characterization tool for metal-organic frameworks. *Journal of Physical Chemistry C*, 2007, **111**, P. 15350-6.

[39] Nicholson D., Parsonage, N.G. *Computer Simulation and the Statistical Mechanics of Adsorption.* Academic, editor. San Diego, 1982.

[40] Farha O.K., Eryazici I., Jeong N.C., Hauser B.G., Wilmer C.E., Sarjeant A.A., et al. Metal–Organic Framework Materials with Ultrahigh Surface Areas: Is the Sky the Limit? *Journal of the American Chemical Society*, 2012, **134**(36), P. 15016-21.

[41] Zhou W., Wu H., Hartman M.R., Yildirim T. Hydrogen and Methane Adsorption in Metal–Organic Frameworks: A High-Pressure Volumetric Study. *The Journal of Physical Chemistry C*, 2007, **111**(44), P. 16131-7.

[42] Wu H., Zhou W., Yildirim T. Methane Sorption in Nanoporous Metal–Organic Frameworks and First-Order Phase Transition of Confined Methane. *The Journal of Physical Chemistry C*, 2009, **113**(7), P. 3029-35.

[43] Furukawa H., Yaghi O.M. Storage of Hydrogen, Methane, and Carbon Dioxide in Highly Porous Covalent Organic Frameworks for Clean Energy Applications. *Journal of the American Chemical Society*, 2009, **131**(25), P. 8875-83.

[44] Dietzel P.D.C., Besikiotis V., Blom R. Application of metal-organic frameworks with coordinatively unsaturated metal sites in storage and separation of methane and carbon dioxide. *Journal of Materials Chemistry*, 2009, **19**(39), P. 7362-70.

[45] Guo Z., Wu H., Srinivas G., Zhou Y., Xiang S., Chen Z., et al. A Metal–Organic Framework with Optimized Open Metal Sites and Pore Spaces for High Methane Storage at Room Temperature. *Angewandte Chemie International Edition*, 2011, **50**(14), P. 3178-81.

[46] Duan X., Yu J., Cai J., He Y., Wu C., Zhou W., et al. A microporous metal-organic framework of a rare sty topology for high CH_4 storage at room temperature. *Chemical Communications*, 2013, **49**(20), P. 2043-5.

[47] Ma S., Sun D., Simmons J.M., Collier C.D., Yuan D., Zhou H.-C. Metal-Organic Framework from an Anthracene Derivative Containing Nanoscopic Cages Exhibiting High Methane Uptake. *Journal of the American Chemical Society*, 2007, **130**(3), P. 1012-6.

[48] Yang Q., Guillerm V., Ragon F., Wiersum A.D., Llewellyn P.L., Zhong C., et al. CH_4 storage and CO_2 capture in highly porous zirconium oxide based metal-organic frameworks. *Chemical Communications*, 2012, **48**(79), P. 9831-3.

[49] Zhao Z., Li Z., Lin Y.S. Adsorption and Diffusion of Carbon Dioxide on Metal–Organic Framework (MOF-5). *Industrial & Engineering Chemistry Research*, 2009, **48**(22), P. 10015-20.

[50] Peng Y., Krungleviciute V., Eryazici I., Hupp J.T., Farha O.K., Yildirim T. Methane Storage in Metal–Organic Frameworks: Current Records, Surprise Findings, and Challenges. *Journal of the American Chemical Society*, 2013, **135**(32), P. 11887-94.

[51] Walton K.S., Millward A.R., Dubbeldam D., Frost H., Low J.J., Yaghi O.M., et al. Understanding inflections and steps in carbon dioxide adsorption isotherms in metal-organic frameworks. *Journal of the American Chemical Society*, 2008, **130**(2), P. 406.

[52] Li D., Kaneko K. Hydrogen bond-regulated microporous nature of copper complexassembled microcrystals. *Chem Phys Lett.*, 2001, **335**, P. 50-56.

[53] Bourrelly S., Llewellyn P.L., Serre C., Millange F., Loiseau T., Ferey G. Different adsorption behaviors of methane and carbon dioxide in the isotypic nanoporous metal terephthalates MIL-53 and MIL-47. *Journal of the American Chemical Society*, 2005, **127**(39), P. 13519-21.

[54] Furukawa H., Ko N., Go Y.B., Aratani N., Choi S.B., Choi E., et al. Ultrahigh Porosity in Metal-Organic Frameworks. *Science*, 2010, **329**(5990), P. 424-8.

[55] Keskin S. Atomistic Simulations for Adsorption, Diffusion, and Separation of Gas Mixtures in Zeolite Imidazolate Frameworks. *The Journal of Physical Chemistry C*, 2010, **115**(3), P. 800-7.

[56] Yazaydın A.Ö. Screening of metal–organic frameworks for carbon dioxide capture from flue gas using a combined experimental and modeling approach. *J Am Chem Soc.*, 2009, **131**, P. 18198-9.

[57] Bae Y.-S., Hauser B.G., Farha O.K., Hupp J.T., Snurr R.Q. Enhancement of CO_2/CH_4 selectivity in metal-organic frameworks containing lithium cations. *Microporous and Mesoporous Materials*, 2011, **141**(1–3), P. 231-5.